

Considerations for design of future cochlear implant electrode arrays: Electrode array stiffness, size, and depth of insertion

Stephen J. Rebscher, MA; Alexander Hetherington, BS; * Ben Bonham, PhD; Peter Wardrop, FRCS; David Whinney, FRCS; Patricia A. Leake, PhD

Department of Otolaryngology, University of California, San Francisco, CA

Abstract—The level of hearing rehabilitation enjoyed by cochlear implant (CI) recipients has increased dramatically since the introduction of these devices. This improvement is the result of continual development of these systems and the inclusion of subjects with less severe auditory pathology. Developments include advanced signal processing, higher stimulation rates, greater numbers of channels, and more efficient electrode arrays that are less likely to produce insertion damage. New directions in the application of CIs, particularly in combined acoustic and electrical stimulation, and increasing performance expectations will place greater demands on future electrode arrays. Specifically, the next generation of arrays must be reliably inserted without damage, must maintain residual acoustic function, and may need to be inserted more deeply. In this study, we measured the mechanical properties of eight clinical and prototype human CI electrode arrays and evaluated insertion trauma and insertion depth in 79 implanted cadaver temporal bones. We found that the size and shape of the array directly affect the incidence of observed trauma. Further, arrays with greater stiffness in the plane perpendicular to the plane of the cochlear spiral are less likely to cause severe trauma than arrays with similar vertical and horizontal stiffness.

Key words: cochlear implant, electrode, electrode array, electrode design, electrode stiffness, insertion damage, insertion depth, rehabilitation, temporal bone, trauma.

INTRODUCTION

Cochlear implants (CIs) have been used successfully for more than two decades as a rehabilitative aid for severe to profound hearing loss. Over this period, the expectation for increased communication capability with these devices has grown dramatically. The earliest CI recipients reported substantial benefits in lipreading performance and recognition of environmental sounds but little or no recognition of speech using only the auditory information provided by the implant [1]. As multichannel CIs were introduced, several studies demonstrated that subjects using these devices could discriminate speech without assistance from visual cues. Improvement in CI performance has continued to the present; many current CI recipients routinely communicate via the telephone, and congenitally deaf children who are implanted as infants or toddlers often develop language skills sufficient to allow them to attend mainstream schools. With the dramatic success achieved to date, one might ask

Abbreviations: AOS = advance off stylet; CI = cochlear implant; CT = computed tomography; RW = round window; ST = scala tympani; TIFF = tagged image file format; UCSF = University of California, San Francisco.

*Address all correspondence to Alexander Hetherington, Department of Otolaryngology, Box 0526, University of California, San Francisco, San Francisco, CA 94143; 415-476-9060; fax: 415-502-2923. Email: ahetherington@ohns.ucsf.edu

DOI: 10.1682/JRRD.2007.08.0119

what direction future research and development efforts should take to increase the performance of CIs and benefit subjects with a wider range of hearing impairments.

A CI operates as an integrated system that includes one or more microphone inputs, a software-controlled digital signal processor, a transcutaneous link, and an intracochlear stimulating electrode array. In this study, we focus on the mechanical design of the electrode array by evaluating five different devices that have been widely implanted in human subjects and three prototype electrode designs in order to ascertain how specific mechanical properties of each device relate to the incidence of damage.

Three widely accepted goals for the development of future CI electrode arrays are (1) deeper insertion into the scala tympani (ST) to access lower frequency cochlear neurons; (2) greater operating efficiency, defined as a reduction in the stimulus charge required to produce a comfortable loudness level; and (3) reduced intracochlear damage associated with surgical insertion.

Deeper Insertion

CI subject testing and acoustic simulations in hearing subjects have shown that speech recognition is degraded when the frequency bands presented to a listener do not approximate the normal acoustic frequency represented at the cochlear place of stimulation [2–8]. Because the tonotopic locations representing the primary speech formant frequencies are located further along the cochlear spiral, i.e., at lower frequency locations, than most fully inserted implant electrode arrays, a significant mismatch occurs for most users between the processed frequency band assigned to each stimulus channel and the cochlear place that it excites. Thus, electrodes with mechanical characteristics that facilitate deeper insertion may be advantageous.

Until recently, determining the optimum depth of insertion and distribution of processed frequency information has been impeded by the lack of an accurate frequency-position map of the human spiral ganglion as well as the lack of a clinical method to assess where each CI stimulating site is located in relation to that map in an individual subject. Recent studies have determined the relationship between the progression of characteristic frequencies along the basilar membrane [9] and the comparable frequency versus position map of neurons in the spiral ganglion [10–11]. Using a different experimental approach, two recent studies of CI patients with residual

hearing compared the pitch percepts produced by stimulation of individual implant channels with percepts produced by acoustic stimulation of varying frequency in the nonimplanted ear [12–13]. Clinical methods using modern high-resolution imaging methods to better estimate the frequency location of the implanted electrode array in individual subjects have also been proposed [10,14]. These anatomical, psychophysical, and imaging studies should help to direct the development of electrode arrays and fitting techniques that will result in a more accurate correspondence between the frequency spectra of processed sounds and the location of electrical stimulation.

Increased Efficiency

The efficiency of an intracochlear electrode array is assumed to be highest when each stimulating element is positioned close to the site of neural activation. This site of activation is assumed to be the cell bodies of spiral ganglion neurons or, in some cases, surviving peripheral nerve fibers within the osseous spiral lamina. We also presume that the site of functional neural activation partly depends on the duration of deafness and probably shifts gradually from peripheral dendrites in recently deaf subjects or those with residual hearing to the spiral ganglion cell bodies in subjects with the longest history of deafness. In any event, electrode arrays introduced within the past 10 years that are designed to position stimulating contacts near the modiolus appear to operate with lower current thresholds than previous devices that were located closer to the lateral wall of the ST [13,15]. Examples of these perimodiolar electrode arrays include the Cochlear Contour™ and Advanced Bionics HiFocus™ electrode arrays.

Reduced Damage

Trauma to the delicate structures of the inner ear frequently occurs during insertion of CI electrodes [16–31]. This damage ranges from relatively minor displacement of the basilar membrane to severe fracture of the osseous spiral lamina, tearing of the basilar membrane or spiral ligament, and deviation of the electrode path from its intended location in the ST to the overlying scala media and/or scala vestibuli. Even in cases of moderate severity, intracochlear trauma may result in reduced numbers of functional peripheral dendrites or spiral ganglion cells, idiosyncratic distribution of these cells, and large variation in the efficiency of stimulating sites along the length of the implanted array. In addition, damage to the medial

surface of the ST, which separates the ST from the internal auditory meatus, might act as a pathway for infection of the central nervous system.

Factors that may affect the incidence of damage include the mechanical properties of a particular electrode design, variations in the size and shape of each cochlea, and the specific surgical techniques used for insertion. Because damage to intracochlear structures occurs most frequently to the partition above the ST, an electrode array designed to minimize upward bending has been proposed to reduce the incidence and severity of insertion-related damage [32]. A reduction in the incidence of damage with two electrode arrays that were designed with increased vertical stiffness was reported by Wardrop et al. [16]. However, a more comprehensive evaluation of the mechanical characteristics of a wide range of electrode designs and their possible correlation with insertion damage has not been reported.

Skinner et al. clearly documented significant variability in the size of the human ST [33], and this variability may be an important factor associated with the rate of trauma observed for CI electrodes with larger cross-sectional dimensions [16,23–24]. Two current CI manufacturers, Advanced Bionics and Cochlear Limited, have introduced curved electrodes that use an internal stylet to hold the electrode straight during all or part of the insertion process. With both devices, the manufacturers recommend that the electrode and stylet be partially inserted into the ST before the electrode is pushed off of the stylet to its full insertion depth. In this process, the precoiled electrode array returns to a spiral shape intended to facilitate insertion and ultimately position the electrode array near the modiolus. This technique has been termed advance off stylet (AOS). Successful insertion with this procedure requires positioning the tip of the electrode and stylet at the beginning of the first cochlear turn before pushing the electrode off of the stylet. If the electrode is advanced off of the stylet with the tip positioned too close to the cochleostomy, the tightly curved tip of the array may fold back upon itself in the expanded basal cavity of the ST. Conversely, if the straightened electrode and stylet are inserted too far beyond the cochleostomy, the electrode tip will contact the outer wall of the first cochlear turn, possibly resulting in damage to the spiral ligament or upward penetration into the scala vestibuli.

The implications of insertion trauma for subjects with residual hearing may be even more serious than for profoundly deaf CI users, since damage to the organ of

Corti could severely affect the transmission and distribution of acoustic vibration along the basilar membrane. The preliminary success of clinical trials with combined electrical and acoustic stimulation highlights the need to develop electrodes that position stimulating contacts close to the modiolus for increased efficiency and that also have the appropriate mechanical features to ensure atraumatic insertion.

Progress to Date

Manufacturers of CIs have addressed these issues in several different ways with varied success. To date, no single design achieves all three objectives of deeper insertion, proximity to the modiolus, and consistent atraumatic insertion. The goal of the present study is to measure the physical characteristics of several existing and prototype CI electrode arrays and to identify specific design features that directly relate to achieving these objectives.

MATERIALS AND METHODS

In this study, eight different models of electrode arrays were tested in cadaver temporal bones ($n = 79$). The six surgeons participating in the study ranged in experience from those leading large CI programs with many years of experience to two otology fellows who had recently completed training in otology and specific CI training equivalent to the device manufacturers' surgical training course. Each surgeon inserted at least two different electrode array models. The insertion damage observed in previous temporal bone trials with the Cochlear Banded™ (Cochlear Limited; Lane Cove, Australia) ($n = 8$), Cochlear Contour™ (Cochlear Limited) ($n = 18$), Spiral Clarion™ (Advanced Bionics; Sylmar, California) ($n = 8$), and HiFocus II™ with positioner (Advanced Bionics) ($n = 20$) designs have been previously reported by this laboratory [16–17]. In this study, we added the mechanical analysis of these previous four electrodes and the temporal bone data and mechanical analysis of four recently tested electrode arrays to permit a broader comparison of the role of electrode mechanical properties and their effect on the occurrence of intracochlear trauma.

Devices Studied

The electrode arrays evaluated in this study include past, current, and prototype designs produced by three

manufacturers. The specific design and the manufacturer of each array tested are described in **Table 1**. The Banded array, manufactured by Cochlear Limited, and the Spiral Clarion, manufactured by Advanced Bionics, are two of the first-generation multichannel CI electrode arrays introduced in the early 1980s. The Banded design is a tapered straight electrode 20 mm in length with 22 equally spaced ring contacts. The Spiral Clarion electrode array has 16 ball contacts in a spiral-shaped carrier with a total length of 24 mm. The contacts are configured as eight pairs with 2 mm between the center of each pair. One contact of each pair was oriented on the medial side of the electrode carrier toward the position of the spiral ganglion, and the second contact was oriented on the upper surface of the carrier toward the osseous spiral lamina or basilar membrane.

The second generation of electrode arrays, the Contour (Cochlear Limited) and HiFocus II (Advanced Bionics), were designed to increase operating efficiency and channel selectivity by decreasing the distance between the stimulating contacts and the spiral ganglion. To accomplish this goal, the stimulating contacts on both designs are located on the medial surface of the electrode and two very different strategies are used to position the electrode closer to the spiral ganglion in situ. The Contour array is premolded to a spiral shape and held on a straight stylet to facilitate insertion. In contrast, the HiFocus II electrode is a slightly curved array that is pushed into close proximity to the modiolus by a separate silicone positioner attached near the tip of the array.

The trauma and insertion depths measured with trial insertions of the Spiral Clarion ($n = 8$), HiFocus II with positioner ($n = 20$), Banded ($n = 8$), and original Contour ($n = 18$) electrode arrays have been previously reported in detail [16–17]. These data are summarized in this report,

and the electrode arrays are further evaluated by the mechanical stiffness measurement techniques described subsequently.

The Contour Advance™ array (Cochlear Limited) is an updated version of the Contour design; it incorporates a more tapered, softer tip and is specifically designed to be inserted by the AOS technique.

The three other electrodes examined in this study, the Nurobiosys array (Seoul, South Korea) and two Helix™ (Advanced Bionics) designs, are experimental prototypes. The Nurobiosys array is a tapered straight array with 16 ball contacts positioned on the upper surface of the silicone carrier [34]. The Helix and prototype 1 designs are arrays with 16 medial contacts similar to the Advanced Bionics electrode arrays currently in clinical use.

Insertion Protocol and Histology

Details of the protocol for trial insertions and the histological techniques used in this study have been published previously [17]. In brief, human temporal bones were harvested within 24 hours of death and placed in refrigerated 10 percent formaldehyde for 24 hours. After fixation, each temporal bone was rinsed in 0.1 M phosphate buffer and stored in refrigerated buffer until use. Each temporal bone was prepared by a standard surgical approach with posterior tympanotomy. In all cases, the facial recess and facial nerve were preserved to model the realistic surgical constraints present in clinical practice. A 1 to 2 mm cochleostomy was performed anteroinferior to the round window (RW). In some cases, the stapes was removed and lubricant (50% glycerin in water) was injected into the ST according to each surgeon's usual practice. Electrode arrays were inserted via the cochleostomy with the design-specific instruments, if any,

Table 1.
Cochlear implant electrode arrays studied.

Electrode	Manufacturer	Type	Scala Tympani Position	No. Studied
Cochlear Banded™	Cochlear Limited	Straight	Lateral	8
Spiral Clarion™	Advanced Bionics	Spiral	Midscala	8
Cochlear Contour™	Cochlear Limited	Spiral	Perimodular	18
HiFocus II™ with Positioner <400°	Advanced Bionics	Curved with Positioner	Perimodular	14
HiFocus II™ with Positioner >400°	Advanced Bionics	Curved with Positioner	Perimodular	6
Contour Advance™	Cochlear Limited	Spiral	Perimodular	3
Nurobiosys	Nurobiosys	Straight	Lateral	6
Helix™	Advanced Bionics	Spiral	Perimodular	6
Prototype 1	Advanced Bionics	Curved	Midscala	10

supplied by each manufacturer. Each array was inserted to the depth specified by the manufacturer or until the surgeon noted resistance.

After insertion, a plain film radiograph was taken of each implanted temporal bone (**Figure 1**). Depth of insertion was estimated from these X-ray images by using the coordinate system shown in **Figure 1** and previously described by Wardrop et al. [17]. Note that this coordinate system was developed specifically for these temporal bone studies. Recently, several different coordinate systems have been used to describe depth of insertion. In general, if the goal is to estimate the characteristic frequency location for stimulating sites along an electrode array, then logically, the zero or reference point for measurement should be the beginning of the basilar membrane. For practical purposes, this reference point would be the RW in CI subjects evaluated by high-resolution computed tomography (CT). However, because the plain film X-ray images used in this study do not permit accurate identification of the RW, we have reported insertion depth based on the previous method, which defines the 0° reference line as a line through the center of the modiolus parallel to the straight basal segment of the first cochlear turn as shown in **Figure 1**. To compare insertion depth across studies, subtract a correction factor of approximately 30° from the values in this study to derive values comparable to those with the RW as the 0° reference.

As described in the “Introduction” section, the initial insertion depth of the electrode and stylet, i.e., the depth before pushing the array off of the stylet by the AOS technique, may be a critical factor in the incidence of trauma. To measure the variability inherent in estimating this location as a distance from the cochleostomy, we measured the distance from the cochleostomy to the beginning of curvature in the first cochlear turn (shown as “L” in **Figure 1**).

Next, the bone overlying the cochlea was thinned with cutting and diamond burrs, the specimens were dehydrated, and each cochlea was embedded in L.R. White Hard Grade acrylic resin (Electron Microscopy Sciences; Fort Washington, Pennsylvania) or Epotek 301 epoxy resin (Epoxy Technology; Billerica, Massachusetts). Each embedded cochlea was then bisected in the midmodiolar plane with a slow speed saw and diamond slicing blade (Buehler; Lake Bluff, Illinois) and the cut surface was polished with aluminum oxide abrasives. In most specimens, a second perpendicular cut separated the cochlea into quarter sections in order to better visualize the full path of

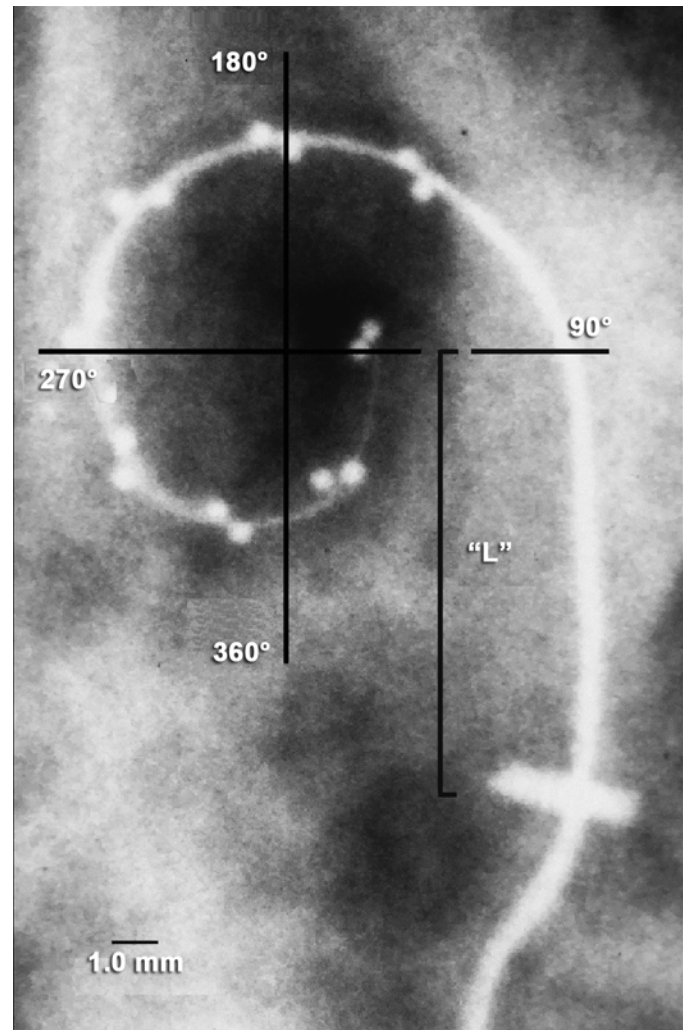


Figure 1.

Plain film X-ray image was obtained for each implanted temporal bone. These images were digitized and insertion angle was measured and tabulated for each electrode array (see main text). Note that this coordinate system differs from those of several other studies that define 0° as line from central axis of cochlea through round window or other location. In addition, relatively straight basal segment of each electrode, i.e., from cochleostomy to point at which electrode clearly begins to curve around cochlear spiral within basal turn, was measured (“L”).

the inserted electrode array. Specimens were evaluated using reflected light and transillumination at magnifications ranging from 8× to 45×. For higher resolution images, 0.5 mm-thick slices were cut with the diamond saw, polished, stained with toluidine blue and basic fuchsin, and digitally imaged using a compound microscope with a combination of incident illumination and transillumination. Damage resulting from electrode insertion was

recorded for each cochlear section. For the purpose of this study, a specimen was considered to have severe trauma if any portion of the electrode had deviated from the ST into the scala media or scala vestibuli with associated fracture of the osseous spiral lamina, tearing of the basilar membrane, or dislocation of the spiral ligament. **Figure 2** illustrates an implanted temporal bone prepared by this method.

Scala Tympani Size and Shape

Clearly, the size and shape of an intracochlear array will have a direct effect on the final position of the array within the ST as well as on the probability of damage associated with insertion. Several temporal bone studies have shown that insertion of a tapered electrode array

may result in severe trauma to the cochlea if the array is inserted past the point where it fills the volume of the ST [16,23–24]. However, few published reports systematically describe the cross-sectional dimensions or shape of the human ST and can act as a guide in the design of intracochlear arrays. To address this need, we measured the ST in 35 of the embedded cochleae used in this study. Temporal bones were selected for these measurements based on two criteria. First, the margins of the ST must be undamaged and clearly visible to ensure accurate measurement. Second, the plane of section for each specimen must be axial to the modiolus. Even though bones were specifically selected for accurate plane of section, we found that maintaining axial orientation near the apex of the cochlea was difficult. For this reason, cross sections

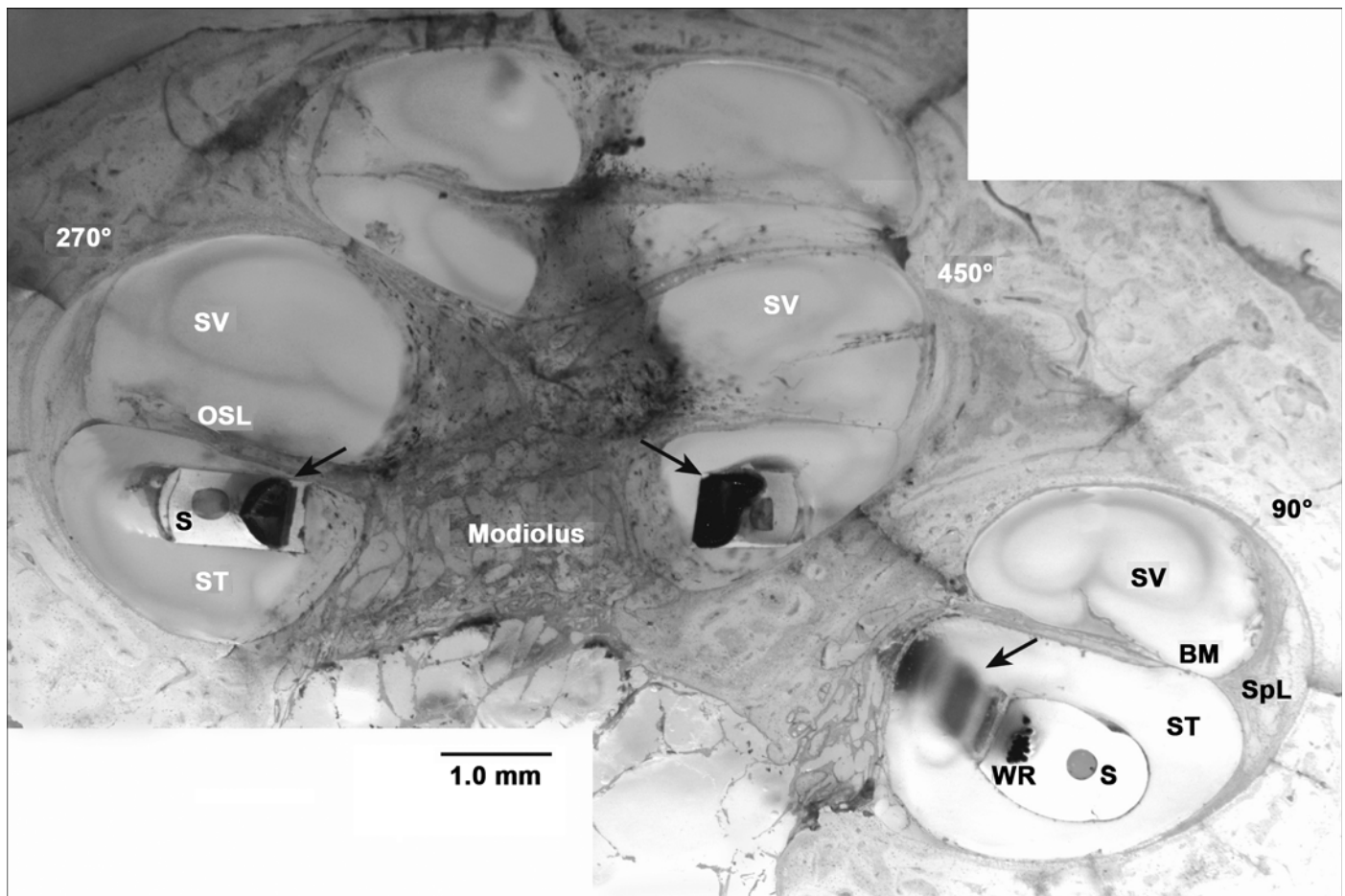


Figure 2.

This montage image illustrates temporal bone implanted with experimental Advanced Bionics Helix™ electrode, embedded in epoxy resin, cut in midmodiolar plane, and stained with toluidine blue and basic fuchsin. Arrows indicate electrode contact sites. BM = basilar membrane, OSL = osseous spiral lamina, S = stylet cavity, SpL = spiral ligament, ST = scala tympani, SV = scala vestibuli, WR = electrode wires.

nearer the apex were eliminated if they appeared to be distorted because of an inaccurate plane of section. This resulted in fewer ST outlines being used for measurements in more apical sections.

To create a database of ST dimensions, we digitally photographed each ST cross section and used Canvas™ imaging software (ACD Systems; Victoria, British Columbia, Canada) to trace the margin of the ST to produce a tagged image file format (TIFF) file. These files were compiled to generate a series of profiles and allow comparison of the varied shape of the ST between individual subjects. Next, to permit statistical analyses of the size, shape, and variation of these ST outlines, we converted each TIFF file to a mathematical format by determining the mean distance from the centroid of the outline to all boundary pixels within each of 64 angular sectors. Visual comparison of the individual traced outlines with the corresponding reconstructed profiles by this method confirmed that this algorithm reliably and accurately described the shape of each ST. Using these data, we calculated the mean ST shape for the group of cross sections at each 90° interval by averaging the distance from the centroid to the profile in each sector and plotting this sector-by-sector average. To illustrate how this method could be used to design the envelope of a CI array, we used the sector-by-sector profile for each ST to estimate the largest circle (i.e., maximum circular carrier cross section) that could lie completely within the ST by using a constrained nonlinear optimization routine (*fmincon*) in MATLAB™ software (The MathWorks, Inc; Natick, Massachusetts).

Measurement of Mechanical Properties

Mechanical properties of the electrode array, including stiffness, also affect the insertion characteristics and final position of the array within the ST. The stiffness of each electrode array design was measured by a custom fixture that securely held the array and a mechanical force gauge that measured the force required to flex the array a total of 30° from its normal shape (**Figure 3**). Stiffness in the vertical and horizontal planes, as defined in the inset in **Figure 3**, was measured at 1 mm increments from the base of the array to the tip. Within each plane, one measurement was made in each direction, i.e., up and down and left and right, and the values measured with two electrode arrays of each design were averaged. The “stiffness ratio” is defined as the ratio of vertical deflection force divided by horizontal deflection force. Because the tip of the electrode array has been reported

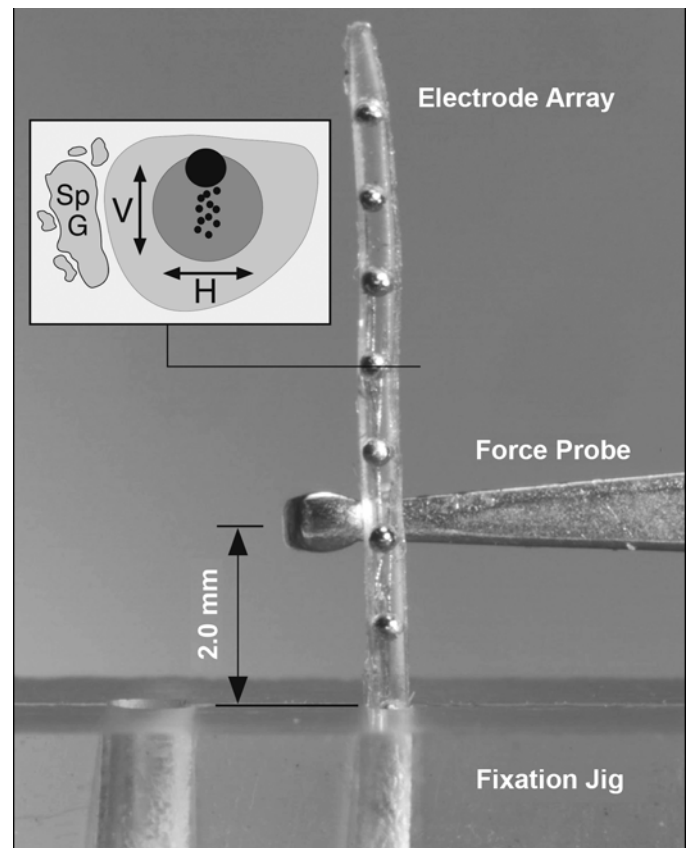


Figure 3.

Deflection force required to bend each electrode array 30° at distance of 2 mm from fulcrum of fixation jig was measured with mechanical force gauge. Deflection force was measured at 1 mm intervals along length of each electrode in both horizontal (H) and vertical (V) planes with respect to intended orientation within scala tympani (as shown in inset). Data from two electrodes were averaged for each design. Image illustrates force probe positioned to measure upward deflection force for straight Nurobiosys electrode array. SpG = spiral ganglion cells.

to be the direct cause of trauma in the majority of specimens with observed damage in previous studies [16–17,19,21–22,35], the stiffness ratio of the terminal 6 mm of each array was used for statistical correlation with damage.

RESULTS

Dimension of Scala Tympani

Figure 4 illustrates the range of size and variation in shape observed in cross sections of the human ST. Sections were cut and imaged at intervals of 90° as shown in the inset schematic for each location (lower right corner

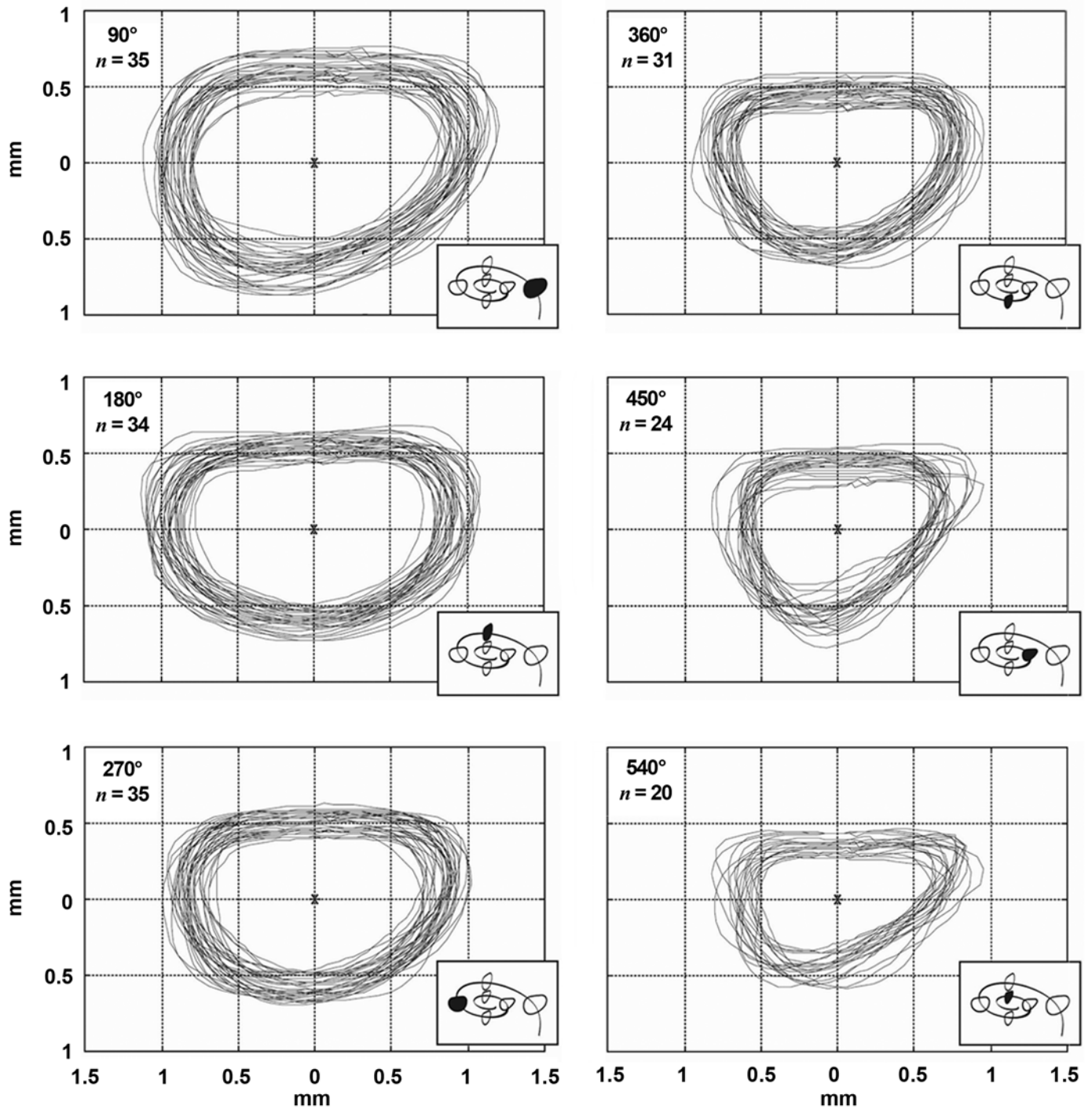


Figure 4.

After epoxy embedding, each temporal bone was cut in midmodiolar plane (and subsequently each half-cochlea was quartered) and digital images were prepared as shown. Outlines of scala tympani were traced at 90° intervals (using Canvas™ software) to provide accurate two-dimensional database to evaluate fit of current and prototype electrode arrays and for use in future cochlear implant design. Group of outlines obtained at each 90° interval were overlaid, with centroid as reference point to align profiles. Only specimens without distortion or damage were selected for measurement. For this reason, number of outlines in database decreases nearer cochlear apex.

of each panel). The maximum size of a circular electrode carrier that could be fit in each cross section was calculated with MATLAB software and tabulated as a frequency histogram in **Figure 5**.

For each 90° interval, we obtained a mean shape of the ST by first dividing each outline from **Figure 4** into 64 angular sectors and then calculating the average radius in each sector. These mean sector radii were assembled to create a mean ST shape for each interval as shown in **Figure 6**.

Advance Off Stylet Insertion

Successful electrode array insertion by the AOS technique requires that the tip of the electrode and stylet be

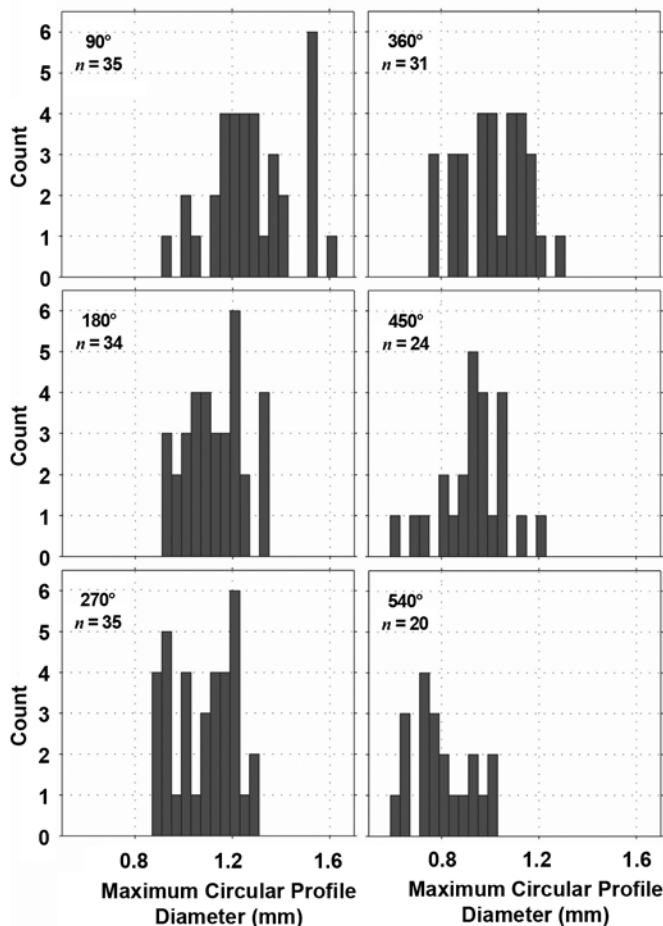


Figure 5.

To assist in design of cochlear implant electrode array, maximum diameter of circular electrode carrier that could fit in each of cross sections shown in **Figure 4** was calculated using MATLAB™ software. These diameters are plotted above as frequency histograms for each 90° interval.

positioned at the beginning of the first cochlear turn before the electrode is pushed off of the stylet. Thus, accurately identifying this position in the clinical setting is important. For this purpose, a marker is provided between the eleventh and twelfth stimulating contact sites on the Contour Advance electrode. With the marker used as a guide during initial insertion of the Cochlear Advance array, the tip of the electrode is located 9 mm into the cochlea when the marker is adjacent to the cochleostomy. To evaluate how the observed anatomic variation in cochlear dimensions might affect the accuracy of this placement technique, we measured the distance from the cochleostomy to the beginning of the first cochlear turn in 62 of these temporal bones. Specimens in which the location of the cochleostomy could not be clearly determined were eliminated for this measurement. This distance (“L” in **Figure 1**) varied from 4.60 to 8.21 mm (mean \pm standard deviation = 6.71 ± 0.82 mm, $n = 62$).

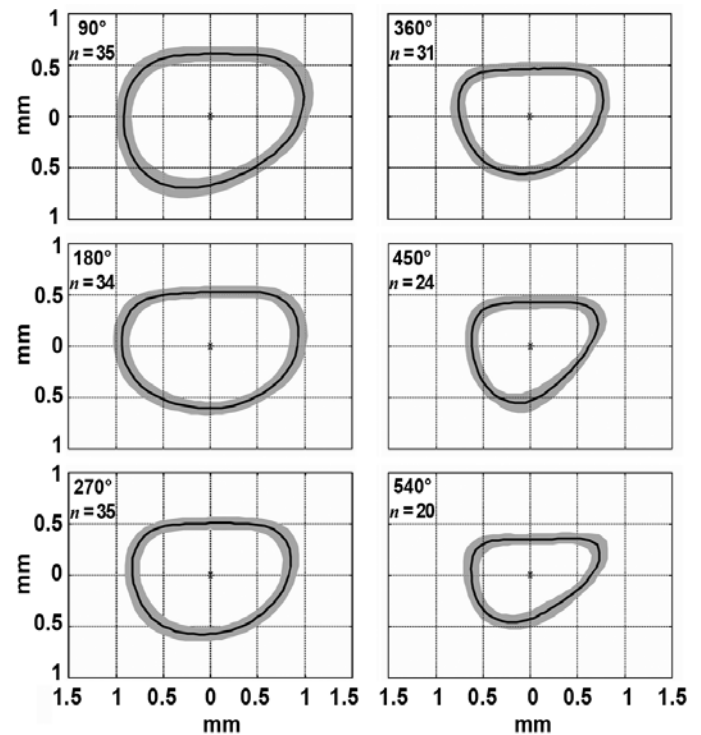


Figure 6.

To determine average human scala tympani shape that would be useful as design tool for future cochlear implant electrode arrays, we used MATLAB™ software to generate mean shape for each 90° interval. Mean cross sections are shown as single dark line surrounded by gray band in each panel. Gray bands represent 1 standard deviation larger and smaller than mean shape.

Insertion Damage and Electrode Stiffness

The stiffness and incidence of insertion trauma resulting in deviation of the electrode array from the ST vertically into the scala media or scala vestibuli are summarized in **Table 2**. Note that no statistically significant difference was seen when we compared the experience of each surgeon with the trauma observed in the temporal bone specimens implanted. Also, the performance of an individual surgeon with one device model did not predict the performance of that surgeon with a different device. For this reason, the results from all surgeons were pooled and results were sorted by electrode array design.

To evaluate the relationship among overall electrode stiffness, differential stiffness ratio (stiffness in the vertical plane divided by stiffness in the horizontal plane), and the resulting insertion damage observed with each electrode design, these factors are plotted in **Figures 7** and **8**.

No statistically significant relationship was seen between mean electrode stiffness and the incidence of severe trauma. However, the ratio of vertical stiffness divided by horizontal stiffness was significantly correlated with the incidence of trauma (Spearman correlation coefficient = -0.83 , $p < 0.01$); i.e., proportionally greater vertical stiffness resulted in significantly less damage. Note that for this analysis we excluded the group of HiFocus II electrodes that were inserted beyond 400° because the high rate of severe damage observed in this group of specimens was clearly due to the size of the electrode with the attached silicone positioner when inserted too deeply and not to the mechanical characteristics of this device.

DISCUSSION

Electrode Array Size

Several neurophysiological studies have reported response thresholds and distribution of evoked neural activity using individual stimulating contact sites or arrays of stimulating contacts held in silicone carriers [36–39]. These studies examined electrodes with and without insulating carriers, with stimulating contacts in different orientations, and with these contacts in varying proximity to the spiral ganglion. They indicate that one factor directly affecting overall efficacy of stimulation is the use of a relatively large nonconductive carrier. Presumably, the reported differences are the result of multiple factors, including reduction in conductive fluid volume surrounding the electrode array and closer positioning of the electrode contacts to the spiral ganglion. From this perspective, the use of a space-filling nonconductive carrier or separately introduced positioner would appear to be a positive design attribute. Based on this principle, larger intracochlear electrode arrays, such as the Advanced Bionics HiFocus array with positioner, and several space-filling prototype arrays were developed.

However, the risk of cochlear trauma during array insertion may be greater with larger volume electrode designs, as reported with the HiFocus II array with positioner [16,23–24]. Nontraumatic implantation requires that the array not be inserted beyond the depth at which the array no longer fits within the tapering ST. In general, experienced CI surgeons have been confident that they could perceive the increase in resistance that presumably precedes insertion damage. However, these recent studies have concluded that even when a careful effort was made

Table 2.
Stiffness measurements, insertion damage, and insertion depth.

Electrode	Force (grams)				Trauma Scala Vestibuli (%)	Mean Depth (°)
	V	H	Mean	V/H		
Cochlear Banded™	0.50	0.70	0.60	0.71	37.5	285
Spiral Clarion™	3.27	2.92	3.09	1.15	0.0	445
Cochlear Contour™	1.33	1.97	1.65	0.68	38.9	417
HiFocus II™ with Positioner <400°	1.29	0.47	0.88	2.77	0.0	332
HiFocus II™ with Positioner >400°	1.29	0.47	0.88	2.77	66.6	508
Contour Advance™	1.33	1.97	1.65	0.68	33.0	367
Nurobiosys	1.03	0.58	0.80	1.77	0.0	360
Helix™ Experimental 1	3.58	1.28	2.43	2.79	0.0	390
Helix™ Experimental 2	3.29	1.23	2.26	2.67	10.0	416

H = horizontal, V = vertical.

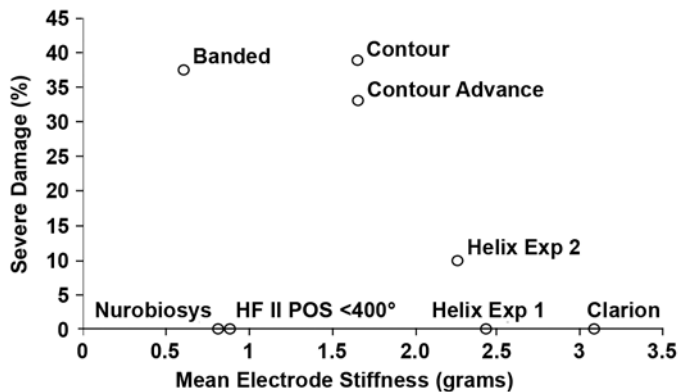


Figure 7.

We measured stiffness of each electrode to correlate specific physical characteristics with insertion damage observed with each electrode type. In analysis shown, incidence of severe trauma resulting in deviation of electrode into scala media or scala vestibuli is plotted as function of mean stiffness (average of vertical and horizontal stiffness measurements). Correlation between these two factors was not statistically significant. Exp = Experimental, HF II POS = HiFocus II with positioner.

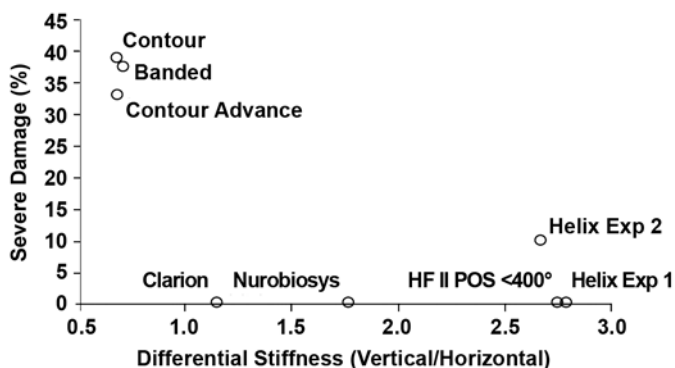


Figure 8.

Incidence of severe trauma is plotted as function of mean differential stiffness (vertical stiffness/horizontal stiffness) for apical 6 mm of each electrode design. Electrode arrays with greater stiffness in vertical plane were less likely to perforate upward into scala media or scala vestibuli than electrodes with isotropic stiffness or greater stiffness in horizontal plane. This result was statistically significant ($p < 0.01$). Exp = Experimental, HF II POS = HiFocus II with positioner.

to stop insertion of the array when resistance was first perceived, severe trauma was frequently observed with larger electrodes [16,23–24]. Based on these reports, the possible advantages of a larger volume nonconductive electrode carrier clearly must be balanced against the increased risk of damage associated with such designs.

Because of the large variation in ST dimensions, future intracochlear electrode arrays must be designed to fit all, or almost all, prospective subjects. Our hope is that the detailed ST dimensional data presented in this report (Figures 4–6) will be useful as a basis for the effective design of these electrode arrays.

With this concern in mind, alternative methods to mechanically position an electrode array closer to the modiolus or, ideally, in gentle contact with the inner wall of the ST should be considered in future designs. To accomplish this goal, most current electrode arrays are molded in a spiral shape designed to match the shape of the modiolar wall. In practice, recent reports illustrate that these arrays are located nearer the center of the ST at many locations along the cochlear spiral. Other approaches might include the ability to change the radius of curvature of the array during or after insertion by using shape memory elastomers or metal alloys, pneumatic or fluidic chambers, or remotely controlled fibers within the carrier. This “steering” capability might be controlled in real time or preprogrammed. Location sensors might be included in the tip of the electrode or stylet or along the length of an array to optimize this capability.

Electrode designs that position the array in contact with the inner (modiolar) wall of the ST may carry increased risk of damage during insertion as a result of the minimal thickness of this structure or erosion of this thin layer of bone in response to chronic localized pressure. In some areas, the inner wall of the ST measures only tens of microns in thickness and represents the only barrier between the fluid-filled volume of the cochlea and the cerebrospinal fluid within Rosenthal’s canal, the internal auditory meatus, and ultimately, the cranial subarachnoid space (Figure 9). Thus, even minor damage to the modiolar wall may cause loss of spiral ganglion cells as a result of direct trauma and could also provide a pathway for the spread of infection from the middle ear, along the CI carrier, and into the cerebrospinal fluid, potentially leading to severe medical complications.

Insertion Depth

In theory, optimum insertion of a CI electrode array would result in a range of perceived frequencies that encompass the spectral range of human speech. Increasing the range of characteristic frequencies activated by these electrode arrays will likely result in improved subject performance both in speech recognition and appreciation of music. In addition to the inclusion of a wider

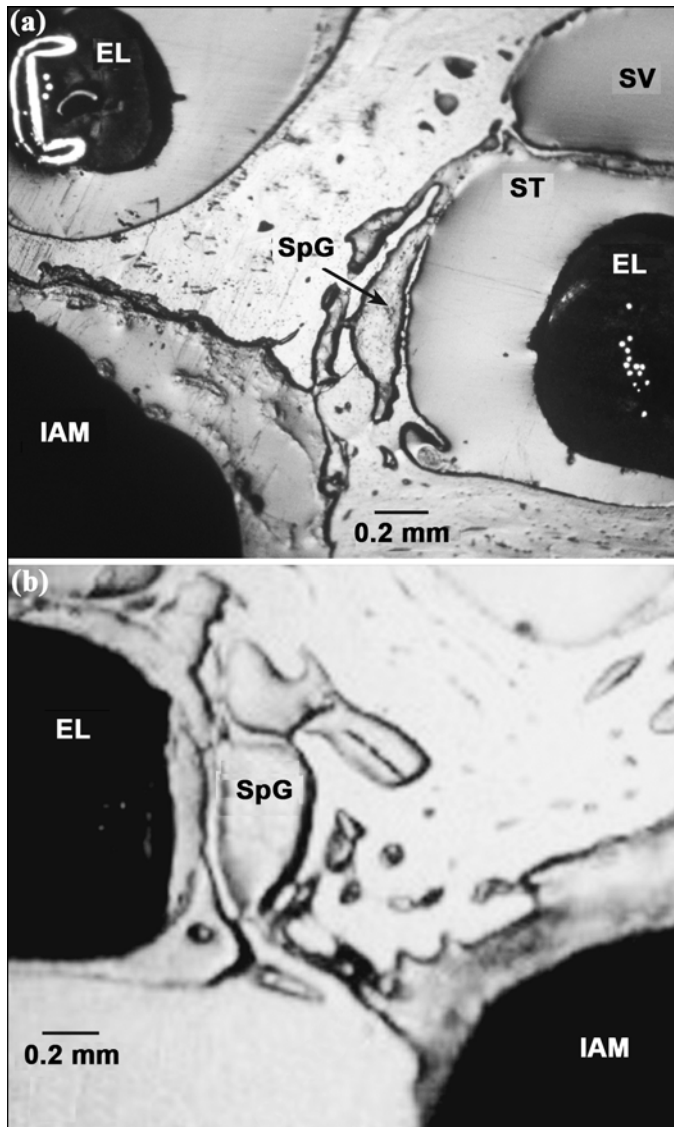


Figure 9.

Inner wall of scala tympani (ST) separates electrode array from spiral ganglion cells (SpG) located in modiolus. These reflected light images of epoxy-embedded human temporal bones implanted with (a) Cochlear Contour™ electrode (labeled “EL”) and (b) Advanced Bionics HiFocus II™ electrode with positioner (labeled “EL”) illustrate thin layer of bone forming this partition and network of fine channels between spiral ganglion and internal auditory meatus (IAM). In (a), basal turn of cochlea is shown at right, with second turn above and to left. Because bone separating ST from IAM is very fragile, damage to this partition during electrode insertion is potential source of serious infection in central nervous system. SV = scala vestibuli.

spectral range of stimulated frequencies, appropriately locating the stimulus frequency bands along the electrode array may also be important. Several previously pub-

lished studies predict that subject performance will improve when the frequency bands of processed speech are delivered to the tonotopically appropriate location in the cochlea [3–4,6–8].

Until recently, no method existed to accurately determine the relationship between the physical location of electrode channels in the ST and the tonotopic frequency of the adjacent location in the spiral ganglion. Stakhovskaya and colleagues provide a map of frequency distribution along the length of the spiral ganglion and insights that may be important in future electrode array design [10].

First, if we assume that the first formant frequencies for human speech are between 200 and 1,200 Hz, this map indicates that the tip of an ideal electrode array would be located near 540° or 1.5 cochlear turns as measured from the RW. In the present study, the mean insertion depth for all electrode designs measured was 391° (approximately 360° measured from the RW) and the mean depth for the perimodiolar electrode designs was 405° (approximately 375° measured from the RW). Thus, we would predict that most subjects using currently available implants would experience some decrement in performance because of a mismatch between the frequency band locations assigned to each CI channel and the tonotopic organization of the spiral ganglion immediately adjacent to these sites.

Second, the spiral ganglion is much shorter than the organ of Corti and the frequency organization of the ganglion is compressed, particularly toward the apex. This compression may make achieving spatial selectivity between apical stimulation channels increasingly difficult. Thus, increased channel interaction may explain, at least in part, the results of psychophysical studies that indicate that the performance increase achieved with very deeply inserted electrodes (up to 720°) is minimal for many subjects [40–41]. In addition, temporal bone studies using deeply inserted electrodes of the same design resulted in significantly increased trauma compared with moderate depth insertions [25]. Thus, the potential increase in channel number and lower frequency channel matching that may be attained with electrode insertions beyond 1.5 turns may not result in an overall increase in patient performance.

With these factors in mind, what is the optimal length for a human CI electrode? We must emphasize that the appropriate measure for frequency location and electrode insertion depth in the cochlea is degrees of rotation. This

measure is critical because of the difference in path length between an electrode array located laterally in the ST and one located closer to the modiolus. As an example, the average length of an electrode array required to reach the 400 Hz location is approximately 25 mm for an array located beneath the organ of Corti (near the inner edge of the basilar membrane) but only 15 mm for an electrode immediately adjacent to the medial wall [10]. Thus, the optimum length for a CI array highly depends on the actual position of the array in situ. Using high resolution CT imaging, one can now estimate both the size of the cochlea in individual subjects preoperatively and the depth of insertion for each electrode array postsurgically [14,33]. This information used in conjunction with the frequency map developed by Stakhovskaya et al. [10] may be a basis for more accurate assignment of frequency bands to stimulation sites during fitting of individual CI users.

Insertion Damage

As shown in **Figure 8**, we found that electrode arrays with proportionately greater stiffness in the vertical plane were less likely to produce severe trauma during insertion. However, no correlation existed between the overall stiffness of the electrode arrays tested and the incidence of damage.

How does electrode array stiffness in the vertical plane affect the incidence of insertion trauma? **Figure 10** illustrates insertion of an electrode array into a dimensionally accurate clear model of the human ST [42]. Although most, but not all, current arrays are molded in a spiral shape, they are inserted with a straight stylet and will contact the outer wall of the ST with a large contact angle very similar to that of a straight array. When this contact occurs, we hypothesize that an array will deviate either in the horizontal plane, the vertical plane, or both, depending on the bending forces inherent in the electrode array. For example, an electrode with greater vertical stiffness will bend in the horizontal plane following the path of least resistance.

In theory, the AOS technique eliminates contact of the precurved array with the outer wall of the first turn because the electrode array is pushed off of the stylet before contact occurs and allows the preformed array to curve toward the modiolus, as illustrated in **Figure 11**. However, if the stylet-mounted array contacts the outer wall before the electrode array is advanced off of the stylet, then the contact with the outer wall is not elimi-

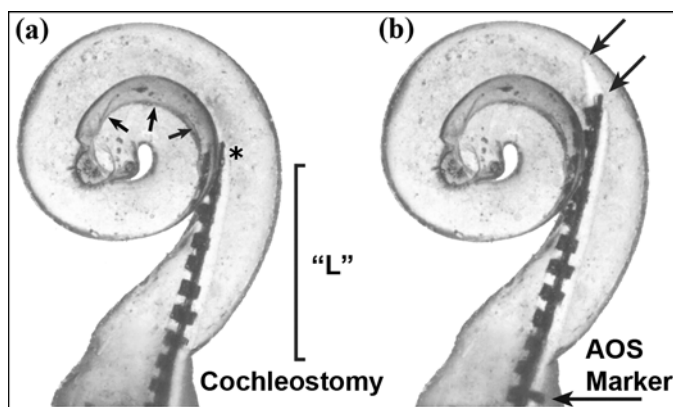


Figure 10.

Initial insertion point for electrode array and stylet using advance off stylet (AOS) technique in dimensionally accurate clear plastic model of human scala tympani. **(a)** If tip of stylet (*) holding spiral molded electrode is placed at point shown, electrode array will curve toward modiolus (small arrows indicate this margin) when it is pushed off of stylet, thus avoiding contact with lateral wall and associated damage. **(b)** However, if stylet and electrode are overinserted during this initial step, tip of electrode and/or stylet (arrows) will contact lateral wall as shown. With this particular replicate model as example, marker included on Contour Advance™ electrode array, which is intended to be positioned at cochleostomy to indicate correct insertion depth for advancing electrode array, is still approximately 1 mm from that location when tip of electrode has contacted lateral wall. We found that this critical distance (“L” in image **(a)** and **Figure 1**) varied by more than 50% in specimens measured in this study. We hypothesize that preoperative measurement, such as high resolution computed tomography imaging, to estimate this distance might significantly reduce incidence of insertion trauma with AOS technique.

nated. As we and others [43] have observed, vertical deflection of the array resulting in penetration of the basilar membrane and/or osseous spiral lamina may still occur with the AOS technique with the latest Cochlear Contour array. We hypothesize that trauma may occur more frequently if the tip of the electrode and stylet are inserted too deeply before the stylet is stabilized and the array pushed off. We found that accurate estimation of the ideal depth for the stylet tip (shown in **Figures 10(a)** and **11**) may be difficult in the clinical setting because of large variation in the distance from the cochleostomy site to the beginning of curvature in the first cochlear turn. In the present study, this critical dimension varied by more than 50 percent of the observed mean value (range = 4.60–8.21 mm, mean = 6.71 mm, $n = 62$). We conclude that an accurate method of determining the optimum depth of stylet placement, e.g., based on preoperative

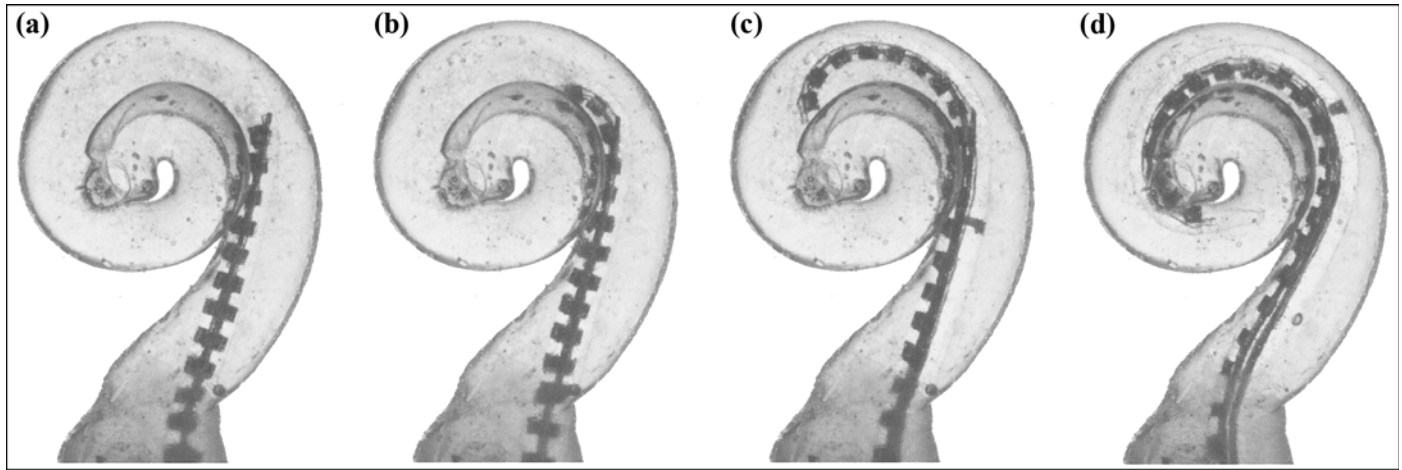


Figure 11.

(a) Intended insertion of spiral molded electrode as it is pushed off of stylet located near beginning of first cochlear turn. (b)–(d) Ideal insertion path of Contour Advance™ electrode array. Tip of electrode resumes its premolded spiral shape as it is pushed off straight stylet and avoids contact with lateral wall. In this particular trial, contact with inner wall was also minimal. Note, however, that achieving this ideal insertion path requires correct placement depth for stylet and electrode and currently no specific effort is made to accurately determine this location in individual patients before implant surgery.

imaging in individual patients, can critically reduce the incidence of damage with the AOS technique.

CONCLUSIONS

The development of improved CI electrode arrays has significantly progressed during the past decade. The results of this study and others demonstrate that newly developed clinical electrode arrays and experimental prototypes are less likely to produce insertion damage than previous models. However, none of the designs evaluated in this study meet all the criteria for an ideal CI electrode: that the electrode be (1) inserted without damage to the cochlea, (2) reliably inserted to a depth of approximately 1.5 cochlear turns (540° as measured from the RW), and (3) positioned near the modiolus for increased efficiency.

We found that the physical characteristics of different electrode designs strongly affected the incidence of insertion trauma observed with each device. First, electrode arrays with overall dimensions that exceeded the volume of the ST were associated with a high rate of trauma even when the surgeon was careful to stop the insertion at the first sense of resistance. Second, electrode designs with greater stiffness in the vertical plane were generally less

likely to produce damage than electrodes that lacked this feature.

In addition to the positive physical characteristics discussed for electrode arrays, we conclude that improvements in surgical methods and insertion instruments are likely to reduce the incidence and severity of trauma during insertion. The rate of damage observed in this study with the Contour Advance array was similar to that seen with earlier versions of the Contour model. However, the sample size in this group was small ($n = 3$) and these trial insertions were performed before the manufacturer's introduction of a prototype insertion tool. A recent study using a larger number of Contour electrodes ($n = 24$) reported a lower incidence of trauma with the Contour Advance design when applied with the AOS technique both with and without the use of the prototype insertion tool [43]. We note that the traumatic insertions documented with the AOS technique in both studies may be due to the large variability in the critical distance from the RW (or cochleostomy) to the beginning of the first cochlear turn. To date, no practical method is used to accommodate this variability during clinical insertion, although preoperative high-resolution CT imaging may offer a solution to this problem.

Looking to the future, we are hopeful that development of CI electrodes will continue to progress toward

optimized devices that meet all the criteria discussed in this study. The increasing number of high-quality temporal bone studies being conducted to evaluate new electrode arrays is providing direction for this effort. However, the engineering challenges to accomplish these goals, including reliably increasing insertion depth without increasing the occurrence of trauma, are substantial and we anticipate that overcoming these obstacles will require innovative new technology.

ACKNOWLEDGMENTS

We would like to thank Dr. Lawrence Lustig (University of California, San Francisco [UCSF]), Dr. William Luxford (House Ear Institute), Dr. J. Thomas Roland Jr (New York University), and Dr. Jose Fayad (House Ear Institute) for their generous contributions of effort to these studies. We would also like to thank Dr. Jafer Ali, Resident in Otolaryngology at UCSF, for his assistance in procuring and preparing temporal bones for these studies. Additionally, we would like to thank the device manufacturers for supplying devices for study, technical assistance, and their ongoing commitment to collaboratively developing improved CI electrode arrays and methods to evaluate their progress.

Dr. Wardrop and Dr. Whinney are currently at the Department of Otolaryngology, Crosshouse Hospital, Kilmarnock, Scotland, and the Department of Otolaryngology, Royal Cornwall Hospital, Truro, England, respectively.

This material was based on work supported by the National Institutes of Health (contract HHS-N-263-2007-00054-C) and by Hearing Research Incorporated. Fellowship support was provided for Dr. Wardrop and Dr. Whinney by the TWJ Foundation, London.

Histological preparation of temporal bone specimens for the Advanced Bionics prototype electrode arrays was supported by Advanced Bionics. Involvement of the manufacturers was limited to this support, the supply of devices for testing, and technical assistance during temporal bone insertions. The manufacturers did not participate in the design of the study, the collection or interpretation of data, the preparation of this article, or the decision to submit this article for publication.

REFERENCES

1. Bilger RC. Evaluation of patients presently fitted with implanted auditory prosthesis. *Ann Otol Rhinol Laryngol.* 1977;87(Suppl 38):1–176.
2. Faulkner A. Adaptation to distorted frequency-to-place maps: Implications of simulations in normal listeners for cochlear implants and electroacoustic stimulation. *Audiol Neurootol.* 2006;11 Suppl 1:21–26. [PMID: 17063007]
3. Fu QJ, Shannon RV. Effects of electrode configuration and frequency allocation on vowel recognition with the Nucleus-22 cochlear implant. *Ear Hear.* 1999;20(4):332–44. [PMID: 10466569]
4. Fu QJ, Shannon RV, Galvin JJ 3rd. Perceptual learning following changes in the frequency-to-electrode assignment with the Nucleus-22 cochlear implant. *J Acoust Soc Am.* 2002;112(4):1664–74. [PMID: 12398471]
5. Oxenham AJ, Bernstein JG, Penagos H. Correct tonotopic representation is necessary for complex pitch perception. *Proc Natl Acad Sci U S A.* 2004;101(5):1421–25. [PMID: 14718671]
6. Baskent D, Shannon RV. Frequency-place compression and expansion in cochlear implant listeners. *J Acoust Soc Am.* 2004;116(5):3130–40. [PMID: 15603158]
7. Baskent D, Shannon RV. Interactions between cochlear implant electrode insertion depth and frequency-place mapping. *J Acoust Soc Am.* 2005;117(3 Pt 1):1405–16. [PMID: 15807028]
8. Baskent D, Shannon RV. Speech recognition under conditions of frequency-place compression and expansion. *J Acoust Soc Am.* 2003;113(4 Pt 1):2064–76. [PMID: 12703717]
9. Greenwood DD. A cochlear frequency-position function for several species—29 years later. *J Acoust Soc Am.* 1990; 87(6):2592–2605. [PMID: 2373794]
10. Stakhovskaya O, Sridhar D, Bonham BH, Leake PA. Frequency map for the human cochlear spiral ganglion: Implications for cochlear implants. *J Assoc Res Otolaryngol.* 2007; 8(20):220–33. [PMID: 17318276]
11. Sridhar D, Stakhovskaya O, Leake PA. A frequency-position function for the human spiral ganglion. *Audiol Neurootol.* 2006;11 Suppl 1:16–20. [PMID: 17063006]
12. Boëx C, Baud L, Cosendai G, Sigrist A, Kós MI, Pelizzone M. Acoustic to electric pitch comparisons in cochlear implant subjects with residual hearing. *J Assoc Res Otolaryngol.* 2006;7(2):110–24. [PMID: 16450213]
13. Dorman MF, Spahr T, Gifford R, Loiselle L, McKarns S, Holden T, Skinner M, Finley C. An electric frequency-to-place map for a cochlear implant patient with hearing in the nonimplanted ear. *J Assoc Res Otolaryngol.* 2007;8(2): 234–40. [PMID: 17351713]

14. Escudé B, James C, Deguine O, Cochard N, Eter E, Fraysse B. The size of the cochlea and predictions of insertion depth angles for cochlear implant electrodes. *Audiol Neurotol.* 2006;11 Suppl 1:27–33. [\[PMID: 17063008\]](#)
15. Cords SM, Reuter G, Issing PR, Sommer A, Kuzma J, Lenarz T. A silastic positioner for a modiolus-hugging position of intracochlear electrodes: Electrophysiologic effects. *Am J Otol.* 2000;21(2):212–17. [\[PMID: 10733186\]](#)
16. Wardrop P, Whinney D, Rebscher SJ, Luxford W, Leake P. A temporal bone study of insertion trauma and intracochlear position of cochlear implant electrodes. II: Comparison of Spiral Clarion and HiFocus II electrodes. *Hear Res.* 2005;203(1–2):68–79. [\[PMID: 15855031\]](#)
17. Wardrop P, Whinney D, Rebscher SJ, Roland JT Jr, Luxford W, Leake PA. A temporal bone study of insertion trauma and intracochlear position of cochlear implant electrodes. I: Comparison of Nucleus Banded and Nucleus Contour electrodes. *Hear Res.* 2005;203(1–2):54–67. [\[PMID: 15855030\]](#)
18. Welling DB, Hinojosa R, Gantz B, Lee JT. Insertional trauma of multichannel cochlear implants. *Laryngoscope.* 1993;103(9):995–1001. [\[PMID: 8361322\]](#)
19. Tykocinski M, Saunders E, Cohen LT, Treaba C, Briggs RJ, Gibson P, Clark GM, Cowan RS. The contour electrode array: Safety study and initial patient trials of a new perimodiolar design. *Otol Neurotol.* 2001;22(1):33–41. [\[PMID: 11314713\]](#)
20. Shepherd RK, Clark GM, Pyman BC, Webb RL. Banded intracochlear electrode array: Evaluation of insertion trauma in human temporal bones. *Ann Otol Rhinol Laryngol.* 1985;94(1 Pt 1):55–59. [\[PMID: 3838226\]](#)
21. Richter B, Aschendorff A, Lohnstein P, Husstedt H, Nagursky H, Laszig R. The Nucleus Contour electrode array: A radiological and histological study. *Laryngoscope.* 2001;111(3):508–14. [\[PMID: 11224784\]](#)
22. Nadol JB Jr, Shiao JY, Burgess BJ, Ketten DR, Eddington DK, Gantz BJ, Kos I, Montandon P, Coker NJ, Roland JT Jr, Shallop JK. Histopathology of cochlear implants in humans. *Ann Otol Rhinol Laryngol.* 2001;110(9):883–91. [\[PMID: 11558767\]](#)
23. Eshraghi AA, Yang NW, Balkany TJ. Comparative study of cochlear damage with three perimodiolar electrode designs. *Laryngoscope.* 2003;113(3):415–19. [\[PMID: 12616189\]](#)
24. Aschendorff A, Klenzner T, Richter B, Kubalek R, Nagursky H, Laszig R. Evaluation of the HiFocus electrode array with positioner in human temporal bones. *J Laryngol Otol.* 2003;117(7):527–31. [\[PMID: 12901805\]](#)
25. Adunka O, Kiefer J. Impact of electrode insertion depth on intracochlear trauma. *Otolaryngol Head Neck Surg.* 2006;135(3):374–82. [\[PMID: 16949967\]](#)
26. Marsh MA, Coker NJ, Jenkins HA. Temporal bone histopathology of a patient with a Nucleus 22-channel cochlear implant. *Am J Otol.* 1992;13(3):241–48. [\[PMID: 1609853\]](#)
27. Fayad J, Linthicum FH Jr, Otto SR, Galey FR, House WF. Cochlear implants: Histopathologic findings related to performance in 16 human temporal bones. *Ann Otol Rhinol Laryngol.* 1991;100(10):807–11. [\[PMID: 1952646\]](#)
28. Fayad JN, Luxford W, Linthicum FH. The Clarion electrode positioner: Temporal bone studies. *Am J Otol.* 2000;21(2):226–29. [\[PMID: 10733188\]](#)
29. Roland JT Jr, Fishman AJ, Alexiades G, Cohen NL. Electrode to modiolus proximity: A fluoroscopic and histologic analysis. *Am J Otol.* 2000;21(2):218–25. [\[PMID: 10733187\]](#)
30. Tykocinski M, Cohen LT, Pyman BC, Roland T Jr, Treaba C, Palamara J, Dahm MC, Shepherd RK, Xu J, Cowan RS, Cohen NL, Clark GM. Comparison of electrode position in the human cochlea using various perimodiolar electrode arrays. *Am J Otol.* 2000;21(2):205–11. [\[PMID: 10733185\]](#)
31. Gstoettner W, Plenk H Jr, Franz P, Hamzavi J, Baumgartner W, Czerny C, Ehrenberger K. Cochlear implant deep electrode insertion: Extent of insertional trauma. *Acta Otolaryngol.* 1997;117(2):274–77. [\[PMID: 9105465\]](#)
32. Rebscher SJ, Heilmann M, Bruszewski W, Talbot NH, Snyder RL, Merzenich MM. Strategies to improve electrode positioning and safety in cochlear implants. *IEEE Trans Biomed Eng.* 1999;46(3):340–52. [\[PMID: 10097469\]](#)
33. Skinner MW, Ketten DR, Holden LK, Harding GW, Smith PG, Gates GA, Neely JG, Kletzker GR, Brunsden B, Blocker B. CT-derived estimation of cochlear morphology and electrode array position in relation to word recognition in Nucleus-22 recipients. *J Assoc Res Otolaryngol.* 2002;3(3):332–50. [\[PMID: 12382107\]](#)
34. An SK, Park SI, Jun SB, Lee CJ, Byun KM, Sung JH, Wilson BS, Rebscher SJ, Oh SH, Kim SJ. Design for a simplified cochlear implant system. *IEEE Trans Biomed Eng.* 2007;54(6 Pt 1):973–82. [\[PMID: 17554817\]](#)
35. Chen BK, Clark GM, Jones R. Evaluation of trajectories and contact pressures for the straight nucleus cochlear implant electrode array—A two-dimensional application of finite element analysis. *Med Eng Phys.* 2003;25(2):141–47. [\[PMID: 12538068\]](#)
36. Van den Honert C, Stypulkowski PH. Single fiber mapping of spatial excitation patterns in the electrically stimulated auditory nerve. *Hear Res.* 1987;29(2–3):195–206. [\[PMID: 3624083\]](#)
37. Rebscher SJ, Snyder RL, Leake PA. The effect of electrode configuration and duration of deafness on threshold and selectivity of responses to intracochlear electrical stimulation. *J Acoust Soc Am.* 2001;109(5 Pt 1):2035–48. [\[PMID: 11386556\]](#)
38. Shepherd RK, Hatsushika S, Clark GM. Electrical stimulation of the auditory nerve: The effect of electrode position

- on neural excitation. *Hear Res.* 1993;66(1):108–20. [\[PMID: 8473242\]](#)
39. Snyder RL, Bierer JA, Middlebrooks JC. Topographic spread of inferior colliculus activation in response to acoustic and intracochlear electric stimulation. *J Assoc Res Otolaryngol.* 2004;5(3):305–22. [\[PMID: 15492888\]](#)
40. Baumann U, Nobbe A. The cochlear implant electrode-pitch function. *Hear Res.* 2006;213(1–2):34–42. [\[PMID: 16442249\]](#)
41. Gani M, Valentini G, Sigrist A, Kós MI, Boéx C. Implications of deep electrode insertion on cochlear implant fitting. *J Assoc Res Otolaryngol.* 2007;8(1):69–83. [\[PMID: 17216585\]](#)
42. Rebscher SJ, Talbot N, Bruszewski W, Heilmann M, Brassell J, Merzenich MM. A transparent model of the human scala tympani cavity. *J Neurosci Methods.* 1996;64(1):105–14. [\[PMID: 8869490\]](#)
43. Stöver T, Issing P, Graurock G, Erfurt P, ElBeltagy Y, Paasche G, Lenarz T. Evaluation of the advance off-stylet insertion technique and the cochlear insertion tool in temporal bones. *Otol Neurotol.* 2005;26(6):1161–70. [\[PMID: 16272935\]](#)

Submitted for publication August 14, 2007. Accepted in revised form March 19, 2008.